https://doi.org/10.5194/tc-2020-87
Preprint. Discussion started: 17 April 2020

The Cryosphere Discussions

Seasonal and Interannual Variability of Melt-Season Albedo at Haig Glacier, Canadian Rocky Mountains

Shawn J. Marshall[1,2] and Kristina Miller[1]

[1] Department of Geography, University of Calgary, Calgary, Alberta, T2N 1N4 Canada
[2] Environment and Climate Change Canada, Gatineau, Quebec, Canada

Correspondence to: Shawn J. Marshall (shawn.marshall@ucalgary.ca)

Abstract. In situ observations of summer albedo are presented for the period 2002-2017 from Haig Glacier in the Canadian Rocky Mountains. The observations provide insight into the seasonal evolution and interannual variability of snow and ice albedo, including the effects of summer snowfall, the decay of snow albedo through the melt season, and the potential short-term impacts of regional wildfire activity on ice albedo reductions. Mean summer albedo (± 1σ) recorded at an automatic weather station in the upper ablation zone of the glacier was α_S = 0.55 ± 0.07 over this period, with no evidence of long-term albedo trends. Each summer the surface conditions at the weather station undergo a transition from a dry, reflective spring snowpack (α_S ~ 0.8), to a wet, homogeneous mid-summer snowpack (α_S ~0.5), to exposed, impurity-rich glacier ice, with a measured albedo of 0.21 ± 0.06 over the study period. The ice albedo drops to ~0.1 during years of intense regional wildfire activity such as 2003 and 2017, but it recovers from this in subsequent years. Summer snowfall events have a significant influence on albedo, and a stochastic parameterization of these events is shown to improve modelled estimates of summer albedo and mass balance. Modifications to conventional degree-day melt factors are also suggested, to better capture the effects of seasonal albedo evolution in climate, hydrology, and glacier mass balance models that use temperature index or positive-degree day methods.

.

1 Introduction

Melting of snow and ice is driven by the net radiative, turbulent, and conductive energy fluxes at the surface. Observations indicate the primary role of absorbed shortwave radiation in driving snow and ice melt on mid-latitude glaciers (Greuell and Smeets 2001; Klok and Oerlemans 2002; Hock 2005; Marshall 2014). Variations in surface albedo therefore exert a strong control on the surface energy balance and available melt energy. This manuscript examines the seasonal variability and multi-year trends in mean melt-season and glacier ice albedo at Haig Glacier in the Canadian Rocky Mountains. Our particular focus is the impact of summer snowfall events, which significantly reduce summer runoff at this site through abrupt, transient increases in albedo. We quantify the average frequency of these events and their impacts on albedo and mass balance at Haig Glacier. We introduce parameterizations of this process for models of glacier energy and mass balance, and also suggest ways

https://doi.org/10.5194/tc-2020-87
Preprint. Discussion started: 17 April 2020

that the net effect of seasonal albedo evolution can be captured in simplified temperature-index melt models, which remain widely used in glaciology (e.g., Marzeion et al., 2014; Clarke et al., 2015; Maussion et al., 2019; Jury et al., 2020).

Seasonal albedo variations are large on mountain glaciers, from ~0.9 for fresh, dry snow (i.e., the spring snowpack, at the start of the melt season), to ~0.5 for aged, wet snow or firn in mid-summer, to as low as 0.1 for impurity-rich glacier ice that is exposed after the seasonal snow has melted (Cuffey and Paterson, 2010). Albedo reductions through the melt season are due to recrystallization to larger, rounded grains, liquid water content in the snow, and increasing concentrations of impurities (Warren and Wiscombe 1980; Wiscombe and Warren, 1980; Marshall and Oglesby 1992; Conway et al., 1996; Gardner and Sharp, 2010).

A representation of this seasonal albedo evolution is important to accurate modelling of glacier melt (e.g., Brock et al., 2000; Klok and Oerlemans 2004). Where direct measurements of albedo are not available, the decrease in supraglacial snow albedo through the melt season is commonly parameterized as a function of snow depth and age (Wigmosta et al., 1994; Oerlemans and Knap, 1998; Klok and Oerlemans 2004) or based on a proxy for cumulative melting, such as cumulative positive degree days (*PDD*) or temperatures above 0°C (e.g., Brock et al., 2000; Bougamont et al., 2005; Hirose and Marshall, 2013). We consider the additional effects of summer snow events on mean melt-season albedo and introduce a simple stochastical method to represent their impact within an empirical albedo parameterization, based on a 14-year record of surface albedo observations at Haig Glacier in the Canadian Rocky Mountains.

Seasonal snow typically melts away by mid- to late-summer on mid-latitude glaciers, exposing low-albedo firn or glacier ice. A wide range of ice albedo values is reported in the literature, from ~0.1 to 0.6 (Bøggild et al., 2010; Cuffey and Paterson, 2010). Lower albedo values are mainly associated with high concentrations of particulate matter on the ice, which can accumulate over many melt seasons. Impurities on mountain glaciers are generally dominated by mineral dust (e.g., Oerlemans et al., 2009; Bühlmann, 2011; Nagorski et al., 2019), but include algae and cyanobacteria (e.g., Takeuchi et al., 2001, 2006; di Mauro et al., 2020; Williamson et al., 2019, 2020), black carbon (soot) and other aerosols from incomplete combustion of fossil fuels, biomass burning, and forest fires (Ming et al., 2009; Keegan et al., 2014; de Magalhães Neto et al., 2019; Nagorski et al., 2019), and other long-range contaminants, such as volcanic dust and heavy metals (e.g., Zdanowicz et al., 2014).

Elevated concentrations of black carbon on glacier surfaces due to increased industrial and wildfire activity have been raised as a concern for glacier mass balance, due to their direct impact on albedo and through melt-albedo feedbacks (Ming et al., 2009; Dumont et al., 2014; Keegan et al., 2014; Mernild et al., 2015; Tedesco et al., 2016; de Magalhães Neto et al., 2019). Similar concerns have been raised about albedo and melt feedbacks associated with algal activity on glaciers (Wientjes and Oerlemans, 2010; Stibal et al., 2017; Williamson et al., 2019; di Mauro et al., 2020). These processes are coupled, as

https://doi.org/10.5194/tc-2020-87
Preprint. Discussion started: 17 April 2020

microbial and algal activity require nutrients and meltwater, which increase in association with greater deposition and concentration of impurities, lower albedo, and longer melt seasons. As an example of nutrient delivery, a classical 'spring bloom' of pink algae (*Chlamydomonas nivalis*) on a glacier can be triggered by walking on a clean, supraglacial snowpack with dirty boots.

In addition, mineral dust deposition on glaciers can increase in association with glacier retreat (Oerlemans et al., 2009), due to exposure of fresh sources of material on the glacier margin as well as melt-concentration effects. Impurities on glacier surfaces are also transported and removed by rainfall and meltwater runoff, as both dissolved and suspended sediment. There is great interest to understand and separate these influences on glacier albedo, to document whether albedo is changing in recent decades, and to quantify the potential impact on glacier mass loss (e.g., Oerlemans et al., 2009; Dumont et al., 2014; Mernild et al., 2015). We examine trends in melt-season and ice albedo at Haig Glacier and discuss the processes governing observed intra- and interannual variations.

A final aim of our study is to examine ways in which the seasonal albedo evolution of mountain glaciers can be implicitly included in temperature-index melt models. Models of snow and ice melt frequently employ simplified parameterizations of melt in mountain and polar environments, where essential meteorological data are neither readily available nor easily modelled (Hock 2005; Fausto et al., 2009). Temperature-index or positive-degree-day methods are the most common approach, with melt parameterized as a function of temperature (e.g., Braithwaite 1984) or from a combination of temperature and potential direct shortwave radiation (Cazorzi and Dalla Fontana 1996; Hock 1999). Snow and ice melt are calculated using a melt factor which linearly relates the amount of melt to cumulative positive degree days and potentially other influences, such as incoming shortwave radiation (Hock, 1999). Melt factors are generally taken as constants for snow and for ice, with a higher value for ice due to its lower albedo. This binary treatment of the melt factor does not realistically represent the continuous nature of surface albedo or the systematic seasonal evolution of albedo and melt rates on a glacier. We therefore explore parameterizations of the melt factor that better capture the effects of the seasonal albedo evolution on modelled melt.

2 Study Site and Methods

2.1 Haig Glacier study site

Glaciological and meteorological measurements at Haig Glacier in the Canadian Rocky Mountains were initiated in August 2000 and are ongoing. Surface energy and mass balance characteristics of this site are summarized in Marshall (2014). Haig Glacier is a moderate-sized (2.62 km^2) outlet of a small icefield that straddles the North American continental divide between British Columbia and Alberta (Figure 1). It flows southeastwards into Alberta and spans an elevation range from about 2520 m at the terminus to 2750 m at the continental divide. Slopes reaching to 2950 m elevation feed into the upper accumulation area. Local geology is dominated by steeply dipping beds of limestone ($CaCO_3$) and dolostone ($MgCO_3$).

https://doi.org/10.5194/tc-2020-87
Preprint. Discussion started: 17 April 2020

The region has mixed continental and maritime influences, being fed by Pacific air masses that transport moisture to the Canadian Rockies (Sinclair and Marshall, 2009). Snow surveys conducted on the glacier each May indicate a mean winter snowpack of 1.35 m water equivalent (w.e.) on the glacier from 2002-2017, with a standard deviation (σ) of 0.24 m w.e. (Table 1). The latter provides a measure of the interannual variability. Summer (June through August (JJA)) temperature on the glacier over the period of study averaged 5.3°C from 2002-2017. The site has warm, sunny conditions in the summer months, driving average summer melt totals ($\pm 1\sigma$) of 2.60 ± 0.62 m w.e over this period. Annual mass balance at the site has been negative in every year of the study (Marshall, 2014; Pelto et al., 2019), with the glacier losing all of its winter snow in 9 of 16 years. Mean annual mass balance over the glacier from 2001-2017 was −1.35 ± 0.24 m w.e., giving a cumulative mean thinning of about 24 m of ice over this period.

Glacier albedo data and meteorological conditions are available from a Campbell Scientific automatic weather station (AWS) installed in the upper ablation zone of the glacier from the period 2001 to 2015. A second AWS was also installed in the glacier forefield in 2001, and remains operational (Figure 1). The stations are maintained through an average of six visits per year, with sensors and dataloggers swapped out four times over the period 2001-2017, to be returned to the University of Calgary weather research station for calibration.

The forefield AWS has been in place continuously, but sensors can fail, the station was blown down once, and on two other occasions the station was buried by snow from the late spring through early summer. Hence there are occasional data gaps, but there is 92% data coverage for the summer period (June through August, JJA) from 2002-2017. Data collection is ongoing at this site. The glacier AWS is more intermittent, due to the more difficult environment. It was maintained year-round from 2001 to 2008, but from 2009 to 2015 the station was set up only in the summer months. It is established at the same site each year. Quality-controlled data represent 79% of JJA days from 2002-2015. Where glacier albedo values are presented in this manuscript, they are restricted to the set of available in situ data. For energy balance and melt modelling, missing glacier meteorological data are estimated from the forefield AWS, with transfer functions (i.e., lapse rates and regression equations) based on the observations that are available from both sites (Marshall, 2014). If data are missing from both stations, gap-filling is based on the mean multi-year value for a given day. This enables a complete estimate of the summer energy and mass balance.

2.2 Field Measurements

AWS data are stored at 30-minute intervals, based on the average of 10-second measurements of temperature, humidity, wind speed and direction, incoming and outgoing longwave and shortwave radiation, rainfall, barometric pressure, and snow/ice

https://doi.org/10.5194/tc-2020-87
Preprint. Discussion started: 17 April 2020

surface height. The AWS observations are subject to a manual quality control, and any questionable data are removed from the analysis. The instrumentation and data are described in more detail in Marshall (2014).

This manuscript concentrates on the long-term albedo record at the glacier AWS site, $\alpha_s = Q_S^{\uparrow}/Q_S^{\downarrow}$, for reflected and incoming shortwave radiation $Q_S^{\uparrow}$ and $Q_S^{\downarrow}$. We have 30-minute values for this, but our pragmatic interest in this study is the seasonal and interannual evolution of surface albedo and its influence on mass balance, so we consider just mean daily albedo, calculated from the integrated daily sum of incoming and outgoing shortwave radiation,

$$\alpha_{sd} = \frac{\int Q_S^{\uparrow} dt}{\int Q_S^{\downarrow} dt}. \quad (1)$$

Note that this gives different values than the average of instantaneous albedo measurements, as it weighs the albedo calculation to the middle of the day, when insolation is highest. This accurately reflects the amount of shortwave energy that is available for glacier melt. It also means that we do not consider zenith angle effects on surface albedo in this study, and measurement uncertainty is reduced through daily averaging. The radiation sensor (Kipp and Zonen CM6B) integrates over the spectral range 0.31 to 2.80 μm, with a manufacturer-reported accuracy of within 5% for mean daily measurements (first class rating from the World Meteorological Organization), although calibration studies indicate mean biases of less than 1% for total daily radiation measurements with this instrument (Myers and Wilcox, 2009). Given that our installation is not maintained on a daily basis and is difficult to maintain an ideal horizontal platform, we take the conservative estimate of an uncertainty of 5% for the mean daily radiation. The uncertainty in mean daily albedo is then 7% (e.g., 0.55 ± 0.04 or 0.20 ± 0.01).

Other sources of uncertainty in the albedo measurements include deviations from horizontality for measurements of incoming shortwave radiation, multiple reflections from the undulating glacier surface, reflected radiation from valley walls, and potential covering of upward-looking sensors during snow events, among other effects. The quality control measures identify obvious environmental corruption such as times when fresh snow is covering the sensors or excessive station leaning, and data from these days are omitted from the analysis. The valley walls are steep and are typically free of snow from July through September, and modelling of potential reflected radiation from valleys walls indicates that this is negligible at our AWS site.

Additional data are included in this paper from summer 2017, based on repeat centreline surveys of albedo and chemical analysis of supraglacial snow and ice. These data, described in detail in Miller (2018), provide an additional spatial perspective on Haig Glacier albedo as well as insights about the provenance and concentration of impurities on the glacier surface and their association with albedo. Four surveys were conducted in July and August, 2017, at 33 points on an altitude transect approximating the glacier centreline (see Section 3). Albedo was only measured under clear-sky conditions and within three hours of local solar noon, to minimize the effects of diffuse radiation and high zenith angles. We used a portable pyranometer

https://doi.org/10.5194/tc-2020-87
Preprint. Discussion started: 17 April 2020

(Jaycar QM1582) for these measurements, taking the average of three upward and three downward shortwave radiation measurements at each point. The sensor was held at a height of ~1.1 m above the glacier surface for all measurements. Based on instrumental fluctuation and repeatability, we assign an uncertainty of 10% to individual radiation measurements. This giving an estimated uncertainty of 8% for the point albedo measurements. Surface snow and ice samples were collected at every third point and were bagged for melting and major ion and organic carbon analyses. The impurity concentrations are referenced here but will be analyzed in detail elsewhere; Miller (2018) provides a complete summary of the chemical analyses.

2.3 Energy Balance Model

We use a distributed surface energy balance model to examine the influence of seasonal and interannual albedo variations on glacier mass balance and summer runoff for the period 2002-2017 (Ebrahimi and Marshall, 2016). We carry out a survey of the winter snowpack each spring, typically in the second week of May, and use this winter mass balance data as an initial condition for the simulation of summer mass balance. The summer melt model is driven by 30-minute data from the glacier AWS; where these data are lacking we drive the melt model with forefield AWS data, mapped onto the glacier through transfer functions that are well-calibrated from the overlapping data records (Marshall, 2014). Four-component radiation measurements, parameterizations of the turbulent fluxes, and a subsurface model of snow/ice temperature and heat conduction (Ebrahimi and Marshall, 2016) are combined to calculate the net surface energy flux, Q_N:

$$Q_N = Q_S^{\downarrow}(1-\alpha_S) + Q_L^{\downarrow} - Q_L^{\uparrow} + Q_H + Q_E + Q_C, \quad (2)$$

where $Q_L^{\downarrow}$, $Q_L^{\uparrow}$, Q_H, Q_E, and Q_C represent incoming and outgoing longwave radiation, sensible and latent heat flux, and subsurface conductive energy flux, respectively. All energy fluxes have units of W m^{-2} and are defined to be positive when they are sources of energy to the surface.

Turbulent fluxes of sensible and latent energy are parameterized from a bulk aerodynamic method (Andreas, 2002; Ebrahimi and Marshall, 2016) and surface temperature and conductive heat flux are internally modelled within a subsurface snow model, which includes calculations of meltwater percolation and refreezing (Samimi and Marshall, 2017). When Q_N is positive and T_s = 0°C, the net energy goes to melting, with melt rate

$$\dot{m} = \frac{Q_N}{\rho_w L_f}, \quad (3)$$

https://doi.org/10.5194/tc-2020-87
Preprint. Discussion started: 17 April 2020

where ρ_w and L_f are the density and latent heat of fusion of water. Melt rates have units m w.e. s^{-1}. By integrating over the time when melt occurs (i.e., when $Q_N > 0$ and $T_s = 0°C$), one can calculate the total melt energy, E_m, over a period of time τ, with units J m^{-2}. Melt over time τ is then calculated from

$$m(\tau) = \frac{E_m}{\rho_w L_f} . \quad (4)$$

This can be directly related to the classical positive degree day method (Braithwaite 1984), where snow or ice melt m over a period of time τ is calculated from

$$m(\tau) = f_{s/i} \int_0^\tau \max(T, 0)\, dt , \quad (5)$$

where $f_{s/i}$ is the degree-day melt factor for snow or ice. This linearly relates the amount of melt to cumulative positive degree days (*PDD*) over time τ. The integrand can also be modified to include other influences, such as the potential direct incoming shortwave radiation (Hock, 1999).

Eq. (5) is an empirical alternative to the physically-based approach in Eq. (4). It is sometimes helpful because surface energy fluxes are uncertain in the absence of local AWS data, due to poorly-constrained meteorological input variables. Wind, humidity, cloud cover, and radiation fields are difficult to estimate in remote mountain terrain. Eq. (5) requires only temperature, which can be estimated via downscaling or interpolation of regional station data or climate model output. While appealing, it is recognized that this parameterization is over-simplified with respect to its transferability to other locations or times. For instance, there is no direct way to incorporate influences from meteorological variables other than temperature, and melt-albedo feedbacks are not physically represented where f_s and f_i are taken as constants.

Most temperature-index models approximate this seasonal evolution to first order by using different melt factors for ice and snow; typical values are f_i ~ 6-9 mm of water equivalent melt per degree day (mm w.e. $°C^{-1}$ d^{-1}), while f_s ~ 3-5 mm w.e. $°C^{-1}$ d^{-1} (Braithwaite, 1995; Jóhannesson, 1997; Hock, 2003; Casal et al., 2004; Shea et al., 2009). There is considerable local, regional, and temporal variability in the parameters chosen for different studies, with values sometimes twice as high as this, particularly for glacier ice (see Hock, 2003). Lefebre et al. (2002) also find a large spatial variation in melt factors, through modelling studies of melt patterns in Greenland. This variability is associated with differences in the energy balance and surface conditions that drive melt, much of which may be due to variations in surface albedo.

For regions where melting is the dominant process in glacier ablation (cf. Lett et al., 2019), one relatively simple way to improve on temperature-index models is to permit melt factors to vary in space and time, consistent with spatial and temporal

https://doi.org/10.5194/tc-2020-87
Preprint. Discussion started: 17 April 2020

variations in net energy and glacier albedo (Schreider et al., 1997; Arendt and Sharp, 1999). For melting over time τ, one can combine Eqs. (4) and (5) to derive an expression for the melt factor at any location (*x*, *y*):

$$f(x,y,\tau) = \frac{E_m(\tau)}{\rho_w L_f \int_0^\tau \max(T,0)\, dt}\,. \quad (6)$$

Eq. (6) implicitly includes the seasonal evolution of surface albedo, as an important control on the melt energy, but numerous other meteorological influences are embedded in E_m, so there is not a direct relation between $f(t)$ and $\alpha_S(t)$. Because absorbed shortwave radiation is the dominant term driving ablation of mountain glaciers (Greuell and Smeets, 2001; Klok and Oerlemans, 2002), including Haig Glacier (Marshall, 2014), one can expect that $E_m \propto 1/\alpha_S$. Moreover, melt energy is proportional to *PDD*, such that the numerator scales with the denominator in Eq. (6). Hence, it should be possible to develop a simple parameterization which includes the lead-order effects of surface albedo on the melt factor. We use Eq. (6) to calculate the seasonal evolution of the melt factor, $f(t)$, at the Haig Glacier AWS site. A compilation of monthly mean values of f and α_S then informs a relation $f = a - b\alpha_S$ which can better represent the seasonal and spatial evolution of melt factors, where albedo is known or can be estimated.

3 Results and Analysis

3.1 AWS Albedo Measurements, 2002-2015

Table 1 gives summary statistics for the observed Haig Glacier mass balance, net energy, and mean summer albedo at the AWS site from 2002-2015. Positive degree day and melt totals are presented for the complete summer melt season, May through September, and temperatures, energy fluxes, and albedo values are given for the core summer months, June through August (JJA), when more than 80% of the melt occurs. Table 2 reports the mean monthly values at the AWS site for the 14-year record.

The mean JJA surface albedo at the AWS site is 0.55, with a marked decrease through the summer months and a minimum of 0.38 in August (Figure 2a). The AWS site is in the upper ablation zone of the glacier, and seasonal snow gives way to bare glacier ice at some point in late summer. This is attended by a sharp drop in albedo, to the bare-ice value of 0.21 ± 0.06. Mean August albedo values represent an average of aged, wet snow and bare ice, with year-to-year variability associated with the timing of seasonal snow depletion. The average date of seasonal snow depletion at the AWS site is August 3, ranging from July 21 to August 20 over the study period. New snow accumulation at the AWS site ('winter snow') begins in September in most years, accounting for the albedo increase this month (Table 2). Persistent snow began to accumulate at the AWS site between August 30 and September 25 during our study period. On average, there are 25 ± 10 days with glacier ice exposed at the AWS site during the melt season. The site was selected because it is near the equilibrium mass balance point of the glacier:

https://doi.org/10.5194/tc-2020-87
Preprint. Discussion started: 17 April 2020

the elevation at which annual snow accumulation is equal to summer melt, for the glacier to be in balance. The observations of bare ice exposure are consistent with the persistent negative mass balance of the glacier over the period of observations.

Intermittent summer snow events also temporarily refresh the glacier surface (*e.g.*, Figure 2b), reducing the number of snow-free days on the glacier surface. The average melt-season albedo evolution at the site in Figure 2a averages out the impact of episodic summer snowfall events that refresh the snow or ice surface (*cf.* Figure 4d). As seen in Figure 2b, these cause an immediate increase in albedo to a fresh-snow value of ~0.9, followed by a decay back to the albedo of the underlying surface over the course of hours to a few days. Figure 3 provides a more detailed illustration of summer snowfall events over exposed glacier ice. This plot covers the period August 3-28, 2015, during which there were three distinct summer snow events, each of which increased the surface albedo for two to three days. The events can be predicted somewhat from the meteorological conditions, where temperature drops below 0°C and relative humidity reaches 100% (Figures 3a,b), but they are most clearly evident in the albedo record (Figure 3c). The accumulation of new snow is also apparent in the glacier surface height (SR50) data (Figure 3d), attended by an interruption in surface melting.

Even a modest amount of fresh snow has a strong albedo impact; there were roughly 4 cm of accumulation in the first two snow events and 8 cm for the third event in Figure 3. The latter event had a longer impact, roughly three days before the surface albedo returned to values typical of bare ice. Total surface ablation at the AWS site was 1.05 m over this 25-day period (Figure 3d), equivalent to about 0.95 m w.e. Based on the observed bare-ice vs. actual average albedo values over the 25-day period, 0.15 vs. 0.27, we calculate that the snow events reduced the average net energy by 24 W m^{-2}, equivalent to 0.16 m w.e. or a 17% reduction in melting over this period. Hence, the direct impact of summer snowfall on glacier mass balance is generally minor (estimated at ~0.03 m w.e. for the events in Figure 3), but the indirect impact through increased albedo and reduced melting is important.

Based on analysis of the SR50 and albedo data over the full study period, an average of 9.3 ± 2.6 ephemeral snowfall events per year occurred at the AWS site from May to September. This included 6.3 ± 2.2 summer (JJA) events. Our main criteria to identify summer snowfall events is a mean daily albedo jump of at least 0.15. This may not capture trace precipitation events that are too minor to be seen in either of the SR50 or albedo measurements (i.e., too ephemeral or not enough snow to mask the underlying surface).

3.2 Relation Between Summer Albedo and Mass Balance

The broader relations between glacier mass balance and albedo, summer snow events, and temperature at the Haig Glacier AWS site are summarized in Table 3. The bottom left portion of the table shows correlation coefficients for monthly mean values (N = 70), while the top right gives mean values for the summer melt-season and annual mass balances (N = 14). Most

https://doi.org/10.5194/tc-2020-87
Preprint. Discussion started: 17 April 2020

variables in Table 3 are correlated, with numerous interactions, but the importance of albedo is clear. Monthly mean albedo is highly correlated with monthly melt (r = –0.89) and net energy (r = –0.84), in addition to strong negative correlations with other melt indicators such as mean monthly temperature and *PDD* (r = –0.74). Monthly albedo values are also significantly correlated with the optimal monthly degree-day melt factor calculated from Eq. (6) (r = –0.66), which we discuss further in Section 4.2.

Correlation coefficients for the mean summer conditions are generally weaker, though there are fewer samples so these statistics are less robust. Mean melt-season albedo remains strongly correlated with summer mass balance (melt), net energy, and temperature, but is only weakly associated with total melt-season *PDD*. The influence of winter mass balance is also evident through positive correlations with albedo and net mass balance; deeper snowpacks take longer to melt out, delaying the transition to the low-albedo summer surface. Mean summer albedo is also positively correlated with the number of summer snow events (r = 0.66). Due to these compounding influences, mean summer albedo is highly correlated with net annual mass balance (r = 0.76). Summer snow events have a significant overall influence on the summer and net mass balance (r = –0.73 and r = 0.70, respectively).

3.3 Ice Albedo Values

The progressive decline in glacier surface albedo through the melt season has been reported in many previous studies (e.g., Brock et al., 2000, Klok and Oerlemans, 2002, 2004). Within the seasonal snow, this can generally be related to cumulative melting, with its associated effects on snow grain size, liquid water content, and increasing concentration of impurities (Warren and Wiscombe, 1980). We discuss modelling of this seasonal evolution in Section 5. At Haig Glacier, the ripened and saturated July snowpack typically asymptotes at an albedo values of about 0.5, before surface albedo drops sharply to a value of ~0.2 once bare ice is exposed. Figure 4a visually captures this transition. The mean glacier albedo value from a composite of 224 bare-ice days in summer (JJA) is 0.21 ± 0.06. Including the month of September, the number of bare-ice days increases to 272 and the mean ice albedo is 0.22 ± 0.07.

Our values for glacier ice albedo are in line with other mid-latitude glacier observations (e.g., Brock et al., 2000; Gerbaux et al., 2005; Naegeli et al., 2019) and the value of 0.2 recommended by Cuffey and Paterson (2010) for impurity-rich ice. Particulate concentrations are high in the old snow and glacier ice on Haig Glacier, and include a combination of mineral dust, black carbon, and organic material (see Section 4.4). Ice albedo values of 0.07 have been measured on the lower glacier in multiple years, in association with high impurity loads (Figure 4b,c). Indeed, during spatial albedo surveys, measured albedo is generally higher on the proglacial limestone than in the lower ablation zone (e.g., Figure 1c and Figure 4b). No part of Haig Glacier is considered to be debris-covered, where material covering the glacier is thick enough to insulate the ice surface from ablation; rather, supraglacial particulate matter takes the form of a thin film, with considerable spatial heterogeneity and

https://doi.org/10.5194/tc-2020-87
Preprint. Discussion started: 17 April 2020

temporal variability in impurity concentrations. The heterogeneity is presumably associated with variable patterns of atmospheric deposition, flushing (cleansing of the glacier surface through rain events or meltwater runoff), and microbial/algal activity. Temporal changes in these processes may underlie the range of ice albedo values measured at the AWS, from 0.11 to 0.34 (Figure 5).

We sorted all bare-ice days into subsets of clear-sky and overcast conditions, based on incoming shortwave radiation measurements at the AWS (specifically, the ratio of the total daily and potential direct incoming solar radiation). The spectral reflectance of snow is dependent on the solar incidence angle (Hubley, 1955; Wiscombe and Warren, 1980), hence differs for direct vs. diffuse radiation. As a result, mean daily albedo values can be expected to be higher on cloudy days, when diffuse radiation is dominant (Cutler and Munro, 1996; Brock, 2004; Abermann et al., 2014). However, we found no difference between the mean ice albedo values for clear-sky and overcast days in our dataset (a mean value of 0.21 for each subset). Glacier ice albedo is less sensitive to the zenith angle than snow (Cutler and Munro, 1996), and this appears to be particularly true for impurity-rich glacier ice, possibly due to isotropic absorption by impurities and liquid water on the glacier surface and in the intergranular interstices.

However, another phenomenon may contribute to some of the higher ice-albedo values recorded at our AWS site. Values above 0.3 are most common in September, after ephemeral snowfall events have melted away; these serve to increase albedo by 0.1 to 0.2 above the minimum seasonal values attained in August. We interpret this to be due to either residual, refrozen (i.e. superimposed) ice that is more reflective or because of meltwater flushing of some of the local impurities. The albedo record in Figure 3c illustrates this temporary increase in albedo in the days following fresh snowmelt, particularly for the third snow event on August 22. The storm snow was melted away by August 24 (Figure 3d), but the exposed ice albedo values remained above their early-August 'baseline' value of ~0.13 until August 28. Albedo values after this returned to the baseline, indicating that a potential crust of superimposed or flushed ice had been melted away. This pattern is typical of the albedo evolution following summer snow events.

Figure 6a plots mean daily ice albedo values through the summer melt season, based on the average of all available data from 2002 to 2015. There is no trend of ice albedo decrease through the summer melt season; hence, no evidence of increasing impurities that cause progressive darkening once the glacier surface ice is exposed. In contrast, ice albedo increases in late August and September, perhaps associated with the brightening influence of superimposed ice or meltwater flushing, as hypothesized above. The summer 2003 was an interesting exception, plotted in red in Figure 6a. Ice albedo declined through July and the first week of August in 2003, reaching a minimum of 0.11 (the lowest mean daily value on record at the Haig AWS) and remaining at ~0.13 until strong melting caused the AWS to lean beyond a condition that ensures reliable data after August 22. Severe wildfire conditions in southwestern Canada that summer resulted in a an evacuation order for the region in

https://doi.org/10.5194/tc-2020-87
Preprint. Discussion started: 17 April 2020

mid-August, so we were forced to leave the site and could not maintain the AWS. These same wildfire conditions may have resulted in deposition of soot and black carbon that produced the extremely low albedo values that summer.

Figure 6b plots the 14-year record of mean and minimum summer albedo at the site for the period 2002-2015. Mean melt-season values are shown for both May through September and JJA. There is interannual variability but not temporal trend to these or to the minimum values over the study period. Notably, the 2003 ice albedo minimum noted above (Figure 6a) was tied for the lowest in the AWS record, matched again in 2015. The ice at the AWS site had a moderately higher albedo in intervening years. The lack of a trend either during the melt season (Figure 6a) or over multiple years (Figure 6b) implies that impurities must be flushed at a rate similar to their concentration through melting, at least in the upper ablation zone.

3.4 Albedo Transects and Snow/Ice Impurity Data

To supplement the AWS albedo record from a single point on the glacier, we conducted spatial albedo surveys across the glacier during different seasons. In summer 2017 we completed four centrelines albedo surveys through July and August, in conjunction with collection of snow and ice samples to analyze the chemistry and concentration of particulate matter on the glacier surface. Figure 7 plots the location of the survey sites and the centreline albedo data from these four surveys, with summary data provided in Table 4.

The characteristic decrease in surface albedo on Haig Glacier over the summer melt season is evident in Figure 7b. For the initial survey on July 13, the glacier surface was still completely snow-covered, with a relatively uniform albedo typical of old, wet snow. The average albedo value (± 1 standard deviation) on the July 13 survey was 0.48 ± 0.04, and albedo declined through each ~two-week period (Table 4). Glacier ice was exposed as the seasonal snowline moved upglacier in the following weeks, with albedo values dropping to 0.16 ± 0.11 on August 22. The toe of the glacier is a high-accumulation area due to wind-blown snow deposition in the lee of a convexity (Adhikari and Marshall, 2013); it retained seasonal snow through mid-August, but was snow-free by August 22. On this final day of sampling, only the uppermost sampling site retained seasonal snow cover, possibly refreshed by a snow event on August 13-14.

The seasonal albedo decline is partly associated with the transition from snow to bare ice and partly because the glacier ice albedo systematically decreased over the course of the melt season, from an average value of 0.21 ± 0.07 on July 25 to 0.13 ± 0.05 on August 22 (Table 4). The snow albedo at the glacier toe also decreased from July 13 to August 9 (Figure 7b), but a decline in snow albedo was not apparent on the upper glacier. Much of the glacier surface had an albedo of ~0.1 by the end of the melt season, and the lower glacier had values of 0.07. As reported in previous studies (Brock et al., 2000; Klok and Oerlemans, 2002), ice albedo generally increases with altitude on Haig Glacier.

https://doi.org/10.5194/tc-2020-87
Preprint. Discussion started: 17 April 2020

These ice albedo values are unusually low compared to values reported in the research literature and in the context of the longer-term record at Haig Glacier. There is an inheritance of accumulated particulate matter on the glacier surface from previous summers, but the significant changes from July 26 to August 22 indicate a strong intra-seasonal change, which feeds back on intensified melting and mass loss through the month of August. Some of this may be due to increasing concentration of impurities, as melting snow and ice leave the particulate load behind while the meltwater runs off. In addition, similar to the summer of 2003, glacier darkening through the month of August may be associated with deposition of soot and other particulate matter associated with regional wildfires. The summer of 2017 was a severe wildfire season in western Canada, with numerous wildfires in southern British Columbia, upwind of Haig Glacier. More than 1.2 million hectares of land burned in the province in 2017, a record at the time (Government of British Columbia, 2020), although this was eclipsed in 2018.

Impurity measurements from snow and ice samples collected during each glacier visit indicate a ~four-fold increase in total carbon on the glacier surface from July 26 to August 9, from average concentrations of 5.6 to 22.7 mg/L, respectively (Miller, 2018). These data will be described in detail elsewhere (Miller and Marshall, in preparation). The increase in impurities was evident in both inorganic and organic carbon, which are present in roughly equal proportions, and are consistent with the potential impacts of wildfire fallout on surface albedo. Particulate matter from local terrigenous dust also increased over this period, but by a factor of about two. The mineral dust load is dominated by calcium and magnesium carbonate, with an average summer carbon concentration associated with carbonaceous dust, [C_{dust}], of 2.2 mg/L. This compares with an average total carbon concentration of 14.5 mg/L, indicating that up to 85% of the carbon on the glacier has a source other than local, terrigenous dust, although we recognize that Ca and Mg are highly soluble and may have been preferentially removed by meltwater. We are not able to partition the non-dust carbon between algal, wildfire, or other potential sources such as British Columbia industrial activity.

4 Discussion

4.1 Albedo Modelling

Given the strong variation of surface albedo through the summer melt season – a typical decline from ~0.9 to ~0.2 from May to August – it is important to capture the seasonal albedo evolution in glacier hydrological and mass balance models. Numerous other researchers have tackled this problem, and physically-based snow albedo models have been proposed (e.g., Marshall and Oglesby, 1994; Flanner and Zender, 2006; Gardner and Sharp, 2010; Aoki et al., 2011).

In glacier modelling, the decrease in supraglacial snow albedo through the melt season can be approximated by a proxy for snow age or cumulative melting, to capture the systematic decline in albedo due to rounding and growth of snow grains, the effects of liquid water content in the snowpack, and increasing concentration of impurities (Brock et al., 2000). Following

https://doi.org/10.5194/tc-2020-87
Preprint. Discussion started: 17 April 2020

Hirose and Marshall (2013), a parameterization based on cumulative *PDD* gives a reasonable fit to observed albedo at Haig Glacier,

$$\alpha_s = \alpha_0 \exp(-k \cdot PDD), \quad (7)$$

where α_0 is the fresh-snow albedo (~0.85) and k is an albedo decay coefficient. The free parameter, k, can be tuned to fit a given observational record such as those plotted in Figure 2b. The influence of snow grain size or impurity concentration could also be incorporated in k in this type of model. Once the seasonal snow has melted, the albedo drops to that of firn or ice. Additional details can be added to the snow albedo model for thin snowpacks (e.g., less than ~10 cm), to capture the influence of the underlying firn or ice albedo when it begins to show through (Oerlemans and Knap, 1998).

This simple parameterization works reasonably well, with minimal inputs, but fails to capture the albedo impact of fresh snow events, which temporarily brighten the glacier surface. The albedo impact of summer snowfall is ephemeral, but these events significantly increase the mean summer albedo and reduce the total summer melt, as discussed in Section 4.2. This is a difficult thing to model remotely or in future projections, as precipitation events can be extremely local in the mountains and the phase of precipitation (rain vs. snow) is difficult to predict. Rain and snow events are both are common on Haig Glacier in the summer months, often mixed on the glacier as a function of elevation.

As a simple approach to address this, we recommend the introduction of summer snow events as a stochastic process. A normal distribution characterized by the mean and standard deviation of the expected number of summer precipitation events (Table 1) can be randomly sampled, with the phase of precipitation determined by the current local temperature (e.g., $T < 2$°C for snowfall). Total event precipitation can also be treated as a random variable. Each summer snow event then resets the surface albedo to the fresh-snow value, α_0, and the albedo decay begins anew with this fresh summer snow, until it is ablated and the underlying, darker surface re-emerges (old snow, firn, or ice). The albedo of the underlying glacier firn or ice can be held constant or can be parameterized to decay with the amount of time exposed or as a function of impurity concentration. Lacking a good understanding or independent model of these processes, we assign the ice albedo to be equal to the observed longterm mean at the Haig Glacier AWS site, 0.21, once again including some stochastic variability based on the observed distribution of ice albedo values (Table 1).

Figure 8 plots an example of this simple treatment for summer 2007, with $k = 0.0009$ (°C d)$^{-1}$. The albedo model is embedded in a glacier energy balance model (Ebrahimi and Marshall, 2016) that calculates *PDD* and melting, forced by the observed AWS data. The model is seeded with the observed winter snowpack, measured on April 13 of that year, and is run from May 1 to September 30. The timing of the transition from seasonal snow to ice is well-captured in Figure 8, and the number of fresh-snow events is also reasonable, but the timing is not correct (nor is it expected to be). Figures 8a and 8b show two

https://doi.org/10.5194/tc-2020-87
Preprint. Discussion started: 17 April 2020

different model realizations, illustrating the differences in timing of summer snow events. These are not completely random, as a stochastic precipitation event will only register as a snowfall when temperatures are cold enough. Because of this, snow events are more common in early and late summer and also correlated in different model realizations. This temperature control also helps the model to capture the end of the summer melt season (beginning of winter snow accumulation), although not always. For instance, the end of summer, which occurs around September 17 this year, is well captured in Figure 8a but is ~one week late in Figure 8b.

4.2 Implications for Glacier Mass Balance

The seasonal albedo decline, summer snow events, and realistic values of firn and ice albedo are all important to resolve in models of glacier energy and mass balance. As an example, the energy balance model driven by the observed AWS meteorological data and surface albedo gives a total melt of 2.97 m w.e. for the 2007 melt season (May to September), the case study in Figure 8, corresponding to a mean surface albedo of 0.59. With the random snow events as illustrated in Figure 8, the mean of five realizations gives an estimated summer melt of 2.82 ± 0.25 m w.e., corresponding to a mean melt-season albedo of 0.60. This slightly underestimates but is within the uncertainty of the observation-based estimate; the energy balance model is well-calibrated to this site. Without the summer snow events, however, modelled melt equals 3.61 m w.e., with a mean melt-season albedo of 0.48. This overestimates summer ablation and runoff by 22%.

There are also important implications for modelling of glacier mass balance at remote sites or in future projections. As temperatures warm, summer precipitation events can be expected to shift to rain rather than snowfall, with positive feedbacks on glacier melting. Without an explicit treatment of summer snow events and their impact on albedo, models calibrated to present-day conditions will not capture this feedback. Similar caveats can be raised about assignment of a constant, observationally-based ice albedo in mass balance models; conditions vary between glaciers and may change in the future as a function of changing particulate loads, and possibly other factors. Physically-based models of impurity deposition and washout and the relation to ice albedo are needed for more reliable regional models and future projections. Similar efforts are underway to improve mass balance models for debris-covered glaciers (e.g., Reid and Brock, 2010; Rowan et al., 2015), although the processes differ for transport and dispersal of coarse debris such as rockfall.

Most studies to date involving regional or future models of glacier mass balance employ degree-day or temperature-index melt models, since in situ meteorological data are unavailable (e.g., Marzeion et al., 2014; Clarke et al., 2015). A full surface energy balance requires a large suite of variables such as wind speed, humidity, and cloud conditions. These are difficult to downscale from climate models with fidelity, relative to temperature fields. In this case, albedo does not appear directly in most formulations of the melt parameterization, but is implicit in the assignment of different degree-day melt factors for snow and ice, f_{snow} and f_{ice}.

https://doi.org/10.5194/tc-2020-87
Preprint. Discussion started: 17 April 2020

Observations of surface albedo evolution on mountain glaciers make it clear that a continuum approach is more appropriate, with changing degree-day melt factors that track the seasonal albedo evolution (e.g., Arendt and Sharp, 1999). The monthly melt factor *f* was calculated from Eq. (6) using mean monthly values of melt energy and temperature at the Haig Glacier AWS from 2002-2015, giving a range of values that can be compared directly with mean monthly albedo (Figure 9). As expected, there is a relatively strong inverse relation, with a linear correlation coefficient of –0.66 and the regression equation $f = 7.98 – 6.16\ \alpha_s$. This relation could be applied if one has independent estimates of the surface albedo, e.g., from remote sensing or UAV surveys. Alternatively, Table 2 includes mean monthly values of the melt factor for the full dataset, which would be preferable to using single values for snow and for ice. Equivalent monthly factors could also be calculated for the radiation melt coefficient in enhanced temperature-index melt models which use potential direct solar radiation as an input (e.g., Hock, 1999; Clarke et al., 2015; Carenzo et al., 2016).

The correlation matrix in Table 3 summarizes the broader relations between albedo, temperature, and mass balance conditions on Haig Glacier. The monthly net energy and melt are strongly correlated with temperature and *PDD* ($r \sim 0.9$), implying that temperature-index melt models could give good estimates of monthly melt at this site, given a judicious choice of melt factor, *f*. This relationship is weaker but still significant for the total summer melt ($r \sim 0.7$). Annual mass balance is highly correlated the summer balance ($r = 0.94$), emphasizing the importance of the summer melt season, which in turn is highly sensitive to surface albedo. Mean summer albedo is highly correlated with net annual mass balance ($r = 0.76$). This is stronger than the correlation of net balance with mean summer temperature or *PDD* totals. Closely related to this, summer snow events have a significant association with the summer and net mass balance ($r = –0.73$ and $r = 0.70$, respectively). The amount of mass added to the glacier is small in summer relative to the winter snowpack (less than 5%), but net mass balance is more strongly correlated with the number of summer snow events than the winter balance, due to the albedo impact.

4.3 Temporal Variability and Trends in Ice Albedo

Glacier ice albedo is low at this site, in association with high concentrations of supraglacial impurities. The impurities are a combination of mineral dust, primarily calcium and magnesium carbonate, other sources of inorganic carbon, and organic carbon, including active algal populations. The mean value of summer ice albedo at the AWS site is 0.21, but this dips to 0.11 in some years (2003, 2015, 2017), possibly in association with regional wildfire activity. The summers of 2003 and 2017 were particularly active wildfire seasons in southern British Columbia, upwind of our study site, and ice albedo declined through the summer melt season in these two summers. This was unusual, however; overall, there is no evidence of decreases in ice albedo over the melt season (Figure 6a). In contrast, bare-ice albedo increases slightly in the late summer and early autumn, perhaps in association with superimposed ice formation and/or meltwater rinsing of the glacier surface after transient summer snow events.

https://doi.org/10.5194/tc-2020-87
Preprint. Discussion started: 17 April 2020

Similarly, there is no multi-year trend for ice albedo at this site (Figure 6b), although this record is limited to a relatively short period (2002-2015) at just one location on the glacier. Based on the available data, however, there is no evidence of glacier 'darkening' over the period of study, despite years such as 2003 which experienced heavy deposition and accumulation of particulate matter. This stands in contrast to reported glacier albedo reductions over the last two decades in other regions (e.g., Mernild et al., 2015; Naegeli et al., 2019). These results imply that there is some degree of effective cleansing and refreshing of the glacier surface through rainfall and meltwater runoff, although the baseline albedo remains low, in connection with a multiyear supraglacial accumulation of impurities.

The transect data from 2017 indicate lower albedo values and greater impurity loads near the glacier terminus (Figure 7b; Miller and Marshall, in preparation). This is consistent with increased concentration of residual particulate matter due to cumulative melting, within a given summer or over many years, as well as the possibility of greater mineral dust loading on the lower glacier (and associated nutrients to support algal activity), as reported by Oerlemans et al. (2009). We do not have the data to assess multiyear albedo or impurity trends on the lower glacier, to test whether the terminus zone is darkening as a feedback to negative mass balance trends, as has been reported elsewhere (Oerlemans et al., 2009; Naegeli et al., 2019).

At a given location on the glacier, increases in concentration of impurities during the melt season generally exceed what would be expected from melt-induced concentration of ions. As an example, at 2730 m altitude in the accumulation area, inorganic carbon concentrations in surface snow increased from 1.4 to 9.1 mg/L from July 26 to August 9, 2017 while calcium concentrations increased from 1.0 to 1.9 mg/L. Melt modelling at this point on the glacier gives an estimated 0.48 m w.e. melt, which should lead to leaching and removal of some dissolved ions in the meltwater runoff, but concentrations increased 2- to 6-fold. Subsurface snow samples were essentially clean (concentrations below the detection limit of 0.1 mg/L), so the increased particulate matter must have been due to deposition on the glacier. Further work is needed to quantify deposition and rinsing (leaching, washout) of particulates, to develop models for these processes, and to characterize their influence on temporal and spatial variations in albedo.

5 Conclusions

Albedo measurements from the upper ablation area of Haig Glacier over the period 2002-2017 indicate significant interannual variability in mean melt-season and glacier ice albedo, but there is no temporal trend in surface albedo over this period. This runs counter to documented albedo reductions elsewhere (Oerlemans et al., 2009; Mernild et al., 2015; Williamson et al., 2019; di Mauro et al., 2020), and to anecdotal evidence of darkening glaciers in the Canadian Rockies. The result may just be specific to the Haig Glacier AWS site; we do not have data to constrain albedo trends on the lower glacier, where changes and melt feedbacks have been strongest over the observation period. Moreover, the record is short for trend detection and Haig Glacier

https://doi.org/10.5194/tc-2020-87
Preprint. Discussion started: 17 April 2020

mass balance has been negative through this whole period. It is plausible that there have not been significant changes in albedo in the 2000s, but there may be substantial darkening over a multi-decadal time frame (e.g., since the 1970s).

The baseline summer ice albedo at the Haig Glacier AWS site is 0.21 ± 0.06, so it has been relatively low for the whole period of study. It drops to values as low as 0.11 in certain years though (2003, 2017), in association with strong wildfire seasons in southern British Columbia, upwind of our study site. Large increases in total and organic carbon concentrations measured on the glacier in August 2017 support this association. The glacier ice appears to recover from these low-albedo summers, however, returning to albedo values of ~0.2 in subsequent years. This is evidence of cleansing of the glacier surface by rainfall and meltwater runoff. Impurities at Haig Glacier are dominated by fine particulate matter, mineral dust in particular and much of this may be effectively leached as dissolved sediment load. The mass balance of supraglacial particulate matter is not well understood, and requires further study.

Other processes controlling the variability in ice albedo also require further study. We find no relation between mean daily ice albedo and cloud conditions in our data, as reported elsewhere (e.g., Brock, 2004; Abermann et al., 2014) and as theoretically expected. This may be because the albedo is relatively low, with a high concentration of impurities; particulate matter and liquid water content act as isotropic absorbers, reducing the sensitivity of specular reflection to zenith angle (hence, diffuse vs. direct radiation). We also see no evidence of ice albedo reductions through the melt season, unlike in seasonal snow, although the major wildfire years provide an exception to this. This further argues for effective rinsing of the glacier surface in most summers, save when dry deposition of particulate matter is unusually high.

We do see evidence of temporary increases in bare-ice albedo to values of ~0.3 following melting and runoff of fresh summer snow. The post-snowfall glacier ice albedo is commonly about 0.15 higher than before the snow event. This may be due to a reflective, superimposed ice crust that temporarily forms after snow events, or it could be a result of effective washing of the glacier surface from the melting of clean snow. The increase in ice albedo is transient, but the effect persists for two or more days after the new snow has melted away.

This effect is subtle, but overall, summer snow events at Haig Glacier have a large impact on mean summer albedo and glacier mass balance. An average of 9.3 ± 2.6 such events were recorded each summer, resulting in a mean melt-season albedo increase of about 0.1 (e.g., from 0.48 to 0.60 in 2007). Such events are particularly significant when they occur late in the summer, temporarily brightening the low-albedo ice. Based on both energy balance modelling and direct AWS observations, we estimate that summer snow events reduce summer melting and runoff by about 20% at Haig Glacier. This is an important potential feedback and sensitivity to climate change, as warming is likely to cause more of these summer precipitation events to shift to rainfall rather than snow in the coming decades.

https://doi.org/10.5194/tc-2020-87
Preprint. Discussion started: 17 April 2020

A stochastic model of summer snow events helps to capture the typical melt-season albedo evolution at Haig Glacier. This is necessary for realistic mass balance modelling at this site, and the approach could be adapted for use elsewhere, with some knowledge of precipitation frequency during the melt season. The seasonal albedo evolution on glaciers governs how effectively incoming shortwave radiation is converted to melt, and it is important to capture this influence in simplified melt and mass balance modelling applications where local meteorological data are not available. We suggest ways in which the melt factor in temperature-index melt models can be parameterized as a function of albedo, to better capture the conversion of positive degree days to melt.

Haig Glacier albedo values and summer snow conditions may not be broadly applicable, particularly given regional differences in the provenance and concentration of impurities. Particulate loading is highly variable in space, even within a given glacier. The processes discussed in this contribution and the general pattern of melt-season albedo evolution are relevant to most mountain glaciers, however. These observations can help to inform regional models of glacier mass balance and assessments of glacier response to climate change. We emphasize the need for process studies of particulate mass balance (deposition, accumulation, transport, and removal) in supraglacial environments, including the potential effects of forest fire fallout on glacier albedo and mass balance.

Acknowledgements

We are grateful to the Natural Science and Engineering Research Council of Canada (NSERC) and the Canada Research Chairs program for sustained, long-term support of the Haig Glacier project. Rick Smith of the University of Calgary Weather Research Station has been instrumental in helping to maintain and calibrate our sensors. Numerous graduate and undergraduate students assisted with the Haig Glacier fieldwork since 2000, and we particularly thank Patrick Coulas for his assistance with the summer 2017 albedo and supraglacial snow/ice sampling.

Code/Data Availability

The automatic weather station data from Haig Glacier and MATLAB code for the surface energy balance model used in this study are available from the authors on request.

Author Contributions

SM initiated the Haig Glacier field study, led the field effort and data collection, wrote the MATLAB code for the surface energy balance modelling, was responsible for the data analysis and wrote the manuscript. KM collected the summer 2017 surface albedo and supraglacial chemistry data as part of her Masters research at the University of Calgary. The authors declare no competing interests and no conflict of interest with this research or its conclusions.

https://doi.org/10.5194/tc-2020-87
Preprint. Discussion started: 17 April 2020

References

Abermann, J., Kinnard, C. and MacDonell, S.: Albedo variations and the impact of clouds on glaciers in the Chilean semi-arid Andes. J. Glaciol., 60 (219), 183-191, 2014.

Adhikari, S. and Marshall, S. J.: Influence of high-order mechanics on simulation of glacier response to climate change: insights from Haig Glacier, Canadian Rocky Mountains, The Cryosphere, 7, 1527–1541, https://doi.org/10.5194/tc-7-1527-2013, 2013.

Andreas, E. L.: Parameterizing scalar transfer over snow and ice: a review, J. Hydrometeorol., 3, 417-432, 2002.

Aoki, T., Kuchiki, K., Niwano, M., Kodama Y., Hosaka M., and Tanaka, T.: Physically based snow albedo model for calculating broadband albedos and the solar heating profile in snowpack for general circulation models. J. Geophys. Res., 116 (D11114), https://doi.org/10.1029/2010JD015507, 2011.

Arendt, A. and Sharp, M. J.: Energy balance measurements on a Canadian high Arctic glacier and their implications for mass balance modelling. IAHS Publ. 256 (Symposium at Birmingham 1999-Interactions between the Cryosphere, Climate and Greenhouse Gases), 165–172, 1999.

Bøggild C. E., Brandt, R. E., Brown K.J., and Warren, S. G.: The ablation zone in northeast Greenland: ice types, albedos and impurities. J. Glaciol. 56 (195), 101-113, 2010.

Bougamont, M., Bamber, J. L., and Greuell, W.: A surface mass balance model for the Greenland Ice Sheet, J. Geophys. Res. Earth Surf., 110, 1–13, https://doi.org/10.1029/2005JF000348, 2005.

Braithwaite, R. J.: Calculation of degree-days for glacier–climate research. Z. Gletscherkd. Glazialgeol., 20, 1-20, 1984.

Braithwaite, R. J.: Positive degree-day factors for ablation on the Greenland ice sheet studied by energy-balance modelling. J. Glaciol., 41 (137), 153-160, 1995.

Brock, B. W.: An analysis of short-term albedo variations at Haut Glacier d'Arolla, Switzerland. Geogr. Ann., 86 (1), 53-65, 2004.

Brock, B. W., Willis, I. C., and Sharp, M. J.: Measurement and parameterisation of albedo variations at Haut Glacier d'Arolla, Switzerland, J. Glaciol., 46, 675-688, 2000.

Bühlmann, E.: Influence of particulate matter on observed albedo reductions on Plaine Morte glacier, Swiss Alps. Unpublished MSc Thesis, University of Bern, Switzerland, 2011.

Carenzo, M., Peilliccioti, F., Mabillard, J. Reid, T. and Brock, B.W.: An enhanced temperature index model for debris-covered glaciers accounting for thickness effect. Adv. Water Resour., 94, 457-469, doi: 10.1016/j.advwatres.2016.05.001, 2016.

Casal, T. G. D., Kutzbach, J. E. and Thompson, L.G.: Present and past ice-sheet mass balance simulations for Greenland and the Tibetan Plateau. Climate Dyn., 23 (3–4), 407–425, 2004.

https://doi.org/10.5194/tc-2020-87
Preprint. Discussion started: 17 April 2020

Cazorzi, F. and Dalla Fontana, G.: Snowmelt modelling by combining temperature and a distributed radiation index. J. Hydrol., 181, 169-187, 1996.

Clarke, G. K. C., Jarosch, A. H., Anslow, F. S., Radić V., and Menounos, B.: Projected deglaciation of western Canada in the twenty-first century, Nat. Geosci. 8, 372-377, 2015.

Conway, H., Gades, A., and Raymond, C. F.: Albedo of dirty snow during conditions of melt. Water Resour. Res. 32, 1713–1718. doi: 10.1029/96WR00712, 1996.

Cuffey, K. M. and Paterson, W. S. B.: The Physics of Glaciers, 4th Ed., 2010.

Cutler, P. M. and Munro, D. S.: Visible and near-infrared reflectivity during the ablation period on Peyto Glacier, Alberta, Canada. J. Glaciol., 42 (141), 333-340, 1996.

de Magalhães Neto, N., Evangelista, H., Condom, T., Rabatel, A. and Ginot, P.: Amazonian biomass burning enhances tropical Andean glaciers melting. Sci. Rep., 9 (16914), 2019.

di Mauro, B., Garzonio, R., Baccolo, G. et al.: Glacier algae foster ice-albedo feedback in the European Alps. Sci Rep, 10, 4739, https://doi.org/10.1038/s41598-020-61762-0, 2020.

Ebrahimi, S. and Marshall, S. J.: Surface energy balance sensitivity to meteorological variability on Haig Glacier, Canadian Rocky Mountains, The Cryosphere, 10, 2799–2819, https://doi.org/10.5194/tc-10-2799-2016, 2016.

Fausto, R. S., Ahlstrøm, A. P., van As, D., Bøggild, C. E. and Johnsen, S. J.: A new present-day temperature parameterization for Greenland. J. Glaciol., 55 (189), 95–105, 2009.

Flanner, M. G., and Zender, C. S.: Linking snowpack microphysics and albedo evolution, J. Geophys. Res., 111, D12208, doi:10.1029/2005JD006834, 2006.

Gardner A. S. and Sharp, M. J.: A review of snow and ice albedo and the development of a new physically based broadband albedo parameterization. J. Geophys. Res., 115 (F01009), doi: 10.1029/2009JF001444, 2010.

Gerbaux, M., Genthon, C., Etchevers, P., Vincent, C. and Dedieu, J. P.: Surface mass balance of glaciers in the French Alps: distributed modelling and sensitivity to climate change. J. Glaciol., 51 (175), 561-572, 2005.

Government of British Columbia, www2.gov.bc.ca/gov/content/safety/wildfire-status/about-bcws/wildfire-statistics, 2019.

Greuell, W. and Smeets, P.: Variations with elevation in the surface energy balance of the Pasterze (Austria). J. Geophys. Res.-Atmos., 106 (D23), 31,717-31,727, 2001.

Hirose, J. M. R. and Marshall, S. J.: Glacier meltwater contributions and glacio-meteorological regime of the Illecillewaet River Basin, British Columbia, Canada, Atmos.-Ocean, 51, 416–435, doi:10.1080/07055900.2013.791614, 2013.

Hock, R.: A distributed temperature-index ice- and snowmelt model including potential direct solar radiation. J. Glaciol., 45 (149), 101-111, 1999.

Hock, R.: Temperature index melt modelling in mountain areas. J. Hydrol., 282 (1–4), 104–115, 2003.

Hock, R.: Glacier melt: a review of processes and their modelling. Prog. Phys. Geog., 29, 362-391, 2005.

Hubley R. C.: Measurements of diurnal variations in snow albedo on Lemon Creek Glacier, Alaska. J. Glaciol., 2 (18), 560-563, doi: 10.3189/002214355793702073, 1955.

Jóhannesson, T.: The response of two Icelandic glaciers to climatic warming computed with a degree-day glacier mass balance model coupled to a dynamic glacier model, J. Glaciol., 43, 321–327, 1997.

Jury, M. W., Mendlik, T., Tani, S., Truhetz, H., Maraun, D., Immerzeel, W. and Lutz, A. F.: Climate projections for glacier change modelling over the Himalayas. Int. J. Climatol., 40 (3), 1738-1754, doi:10.1002/joc.6298, 2020.

Keegan, K. M., Albert, M. R., Mcconnell, J. R. and Baker, I.: Climate change and forest fires synergistically drive widespread melt events of the Greenland ice sheet. Proc. Natl. Acad. Sci. 111, 7964-7967, https://doi.org/10.1073/pnas.1405397111, 2014.

Klok, E. J. and Oerlemans, J.: Model study of the spatial distribution of the energy and mass balance of Morteratschgletscher, Switzerland. J. Glaciol., 48 (163), 505-518, 2002.

Klok, E. J. and Oerlemans, J.: Modelled climate sensitivity of the mass balance of Morteratschgletscher and its dependence on albedo parameterization, Int. J. Climatol., 24, 231–245, 2004.

Lefebre, F., Gallée, H., van Ypersele, J.-P., and Huybrechts, P.: Modelling of large-scale melt parameters with a regional climate model in South-Greenland during the 1991 melt season. Ann. Glaciol. 35, 391-397, 2002.

Litt, M., Shea, J. M., Wagnon, P., Steiner, J., Koch, I., Stigter, E. and Immerzeel, W.: Glacier ablation and temperature indexed melt models in the Nepalese Himalaya. Sci. Rep., 9, 5264, https://doi.org/10.1038/s41598-019-41657-5, 2019.

Marshall, S. and Oglesby, R. J.: An improved snow hydrology for GCMs. Part I: snow cover fraction, albedo, grain size, and age. Clim. Dyn., 10, 21-37, 1994.

Marshall, S. J.: Meltwater runoff from Haig Glacier, Canadian Rocky Mountains, 2002–2013, Hydrol. Earth Syst. Sci., 18, 5181–5200, doi:10.5194/hess-18-5181-2014, 2014.

Marzeion, B., Cogley, J. G., Richter, K., and Parkes, D.: Attribution of global glacier mass loss to anthropogenic and natural causes, Science, 345, 919-921, 2014.

Maussion, F., Butenko, A., Champollion, N., Dusch, M., Eis, J., Fourteau, K., Gregor, P., Jarosch, A. H., Landmann, J., Oesterle, F., Recinos, B., Rothenpieler, T., Vlug, A., Wild, C. T., and Marzeion, B.: The Open Global Glacier Model (OGGM) v1.1, Geosci. Model Dev., 12, 909–931, https://doi.org/10.5194/gmd-12-909-2019, 2019.

Mernild, S. H., Malmros, J. K., Yde, J. C., Wilson, R., Knudsen, N. T., Hanna, E., Fausto, R. S. and van As, D.: Albedo decline on Greenland's Mittivakkat Gletscher in a warming climate. Int. J. Climatol., 35 (9), 2294-2307, 2015.

Ming, J. et al.: Black Carbon (BC) in the snow of glaciers in west China and its potential effects on albedo. Atmos. Res., 92, 114–123, 2009.

Miller, K.: Characterization of meltwater chemistry at Haig Glacier, Canadian Rocky Mountains. Unpublished MSc Thesis, University of Calgary, 2018.

Myers, D. R. and Wilcox, S. M.: Relative accuracy of 1-minute and daily total solar radiation data for 12 global and 4 direct beam solar radiometers. Conference paper NREL/CP-550-45374, American Solar Energy Society, Buffalo, New York, 2009.

Naegeli, K., Huss, M., and Hoelzle, M.: Change detection of bare-ice albedo in the Swiss Alps, The Cryosphere, 13, 397–412, https://doi.org/10.5194/tc-13-397-2019, 2019.

Nagorski, S. A., Kaspari, S. D., Hood, E., Fellman, J. B. and Skiles, S. M.: Radiative forcing by dust and black carbon on Juneau Icefield, Alaska. J. Geophys. Res.-Atmos., 127 (7), 3943-3959, https://doi.org/10.1029/2018JD029411, 2019.

Oerlemans, J., and Knap, W. H.: A 1 year record of global radiation and albedo in the ablation zone of Morteratschgletscher, Switzerland. J. Glaciol. 44 (147), 231–238, 1998.

Oerlemans, J., Giesen, R. and van den Broeke, M. R.: Retreating alpine glaciers: increased melt rates due to accumulation of dust (Vadret de Morteratsch, Switzerland). J. Glaciol. 55, 729-736, 2009.

Rowan, A.V., Egholm, D.L., Quincey, D.J. and Glasser, N. F.: Modelling the feedbacks between mass balance, ice flow and debris transport to predict the response to climate change of debris-covered glaciers in the Himalaya. Earth Planet. Sci. Lett., 430, 427-438, 2015.

Schreider, S.Y., Whetton, P.H., Jakeman, A.J. and Pittock, A.B. 1997: Runoff modelling for snow-affected catchments in the Australian alpine region, eastern Victoria. *Journal of Hydrology* 200, 1–23.

Shea, J. M., Moore, R. D. and Stahl, K.: Derivation of melt factors from glacier mass-balance records in western Canada. J. Glaciol. 55 (189), 123-130, 2009.

Sinclair, K. and Marshall, S.: The impact of vapour trajectory on the isotope signal of Canadian Rocky Mountain snowpacks, J. Glaciol., 55, 485–498, 2009.

Stibal, M., Box, J. E., Cameron, K. A., Langen, P. L., Yallop, M. L., Mottram, R. H., et al.: Algae drive enhanced darkening of bare ice on the Greenland ice sheet. Geophys. Res. Lett. 44, 11,463–11,471, doi:10.1002/2017GL075958, 2017.

Takeuchi, N., Kohshima, S. and Katsumoto, S.: Structure, formation, and darkening process of albedo-reducing material (Cryoconite) on a Himalayan glacier: a granular algal mat growing on the glacier. Arct. Antarct. Alp. Res., 33 (2), 115-122, 2001.

Takeuchi, N., Uetake, J., Fujita, K., Aizen, V., and Nikitin, S.: A snow algal community on Akkem Glacier in the Russian Altai Mountains. Ann. Glaciol. 43, 378–384. doi: 10.3189/172756406781812113, 2006.

Tedesco, M., Doherty, S., Fettweis, X., Alexander, P., Jeyaratnam, J., and Stroeve, J.: The darkening of the Greenland ice sheet: trends, drivers, and projections (1981–2100), The Cryosphere, 10, 477–496, https://doi.org/10.5194/tc-10-477-2016, 2016.

Warren, S. G. and Wiscombe, W. J.: A model for the spectral albedo of snow. II: Snow containing atmospheric aerosols. J. Atmos. Sci., 37, 2734–2745. doi: 10.1175/1520-0469, 1980.

Wientjes, I. G. M., and Oerlemans, J.: An explanation for the dark region in the western melt zone of the Greenland ice sheet. The Cryosphere, 4, 261-268, doi:910.5194/tc-4-261-201, 2010.

Wigmosta, M. S., Vail, L.W. and Lettenmaier, D. P.: A distributed hydrology-vegetation model for complex terrain. Water Resour. Res., 30, 1665-1680, doi:10.1029/94WR00436, 1994.

Williamson, C. J., Cameron, K. A., Cook, J. M., Zarsky, J. D., Stibal, M. and Edwards, A.: Glacier algae: a dark past and a darker future. Front. Microbiol., 10, 524, doi:10.3389/fmicb.2019.00524, 2019.

Williamson, C. J., Cook, J., Tedstone, A., Yallop, M., McCutcheon, J., Poniecka, E., Campbell, D., Irvine-Fynn, T., McQuaid, J., Tranter, M., Perkins, R., Anesio, A.: Algal photophysiology drives darkening and melt of the Greenland Ice Sheet**.** Proc. Nat. Acad. Sci., 201918412 DOI: 10.1073/pnas.1918412117, 2020.

Wiscombe, W. J., and Warren, S. G.: A model for the spectral albedo of snow, I: pure snow. J. Atmos. Sci., 37, 2712–2733. doi: 10.1175/1520-0469, 1980.

Zdanowicz, C., Fisher, D., Bourgeois, J. et al.: ice cores from the St. Elias Mountains, Yukon, Canada: Their significance for climate, atmospheric composition, and volcanism in the North Pacific region. Arctic, 67, 35-57, 2014.

https://doi.org/10.5194/tc-2020-87
Preprint. Discussion started: 17 April 2020

Tables and Figures

Table 1. Mean summer albedo and mass balance conditions at Haig Glacier, 2002-2017, based on glacier-wide simulations driven by local AWS data. B_w, B_s, and B_n are the winter, summer and annual specific mass balance, N_m and N_{ss} are the number of melt days and summer snowfall days from May through September, *PDD* are the positive degree days over the summer melt season, T and Q_N are the mean JJA air temperature and net energy flux, and E_m is the total summer melt energy. Albedo values are as measured at the glacier AWS, where α_S is the mean JJA surface albedo and α_i is the measured ice albedo for the composite of snow-free days (N = 224).

	B_w (m w.e.)	B_s (m w.e.)	B_n (m w.e.)	N_m	N_{ss}	*PDD* (°C d)	T (°C)	Q_N (W m^{-2})	E_m (GJ m^{-2})	α_s	α_i
mean	1.35	–2.60	–1.25	137	9.3	671	5.3	107	1.113	0.55	0.21
std dev	0.24	0.62	0.68	8	2.6	92	0.8	17	0.177	0.07	0.06

Table 2. Mean monthly temperature, surface energy balance, and melt conditions at the Haig Glacier AWS, 2002-2015. Symbols are as in Table 1, with the addition of degree-day melt factors, f_E and f_{PDD}, calculated from Eqs. (6), and (5).

Month	T (°C)	*PDD* (°C d)	Q_N (W m^{-2})	E_m (MJ m^{-2})	α_s	*melt* (m w.e.)	f_E (m w.e. (°C d)$^{-1}$)	f_{PDD}
May	–1.0	42	22	47	0.77	0.13	3.4	3.3
June	2.8	100	62	142	0.71	0.40	4.4	4.2
July	6.8	212	126	319	0.56	0.93	4.5	4.4
August	6.1	191	137	368	0.38	1.10	5.8	5.8
Sept	2.0	91	42	116	0.64	0.35	3.7	3.7

https://doi.org/10.5194/tc-2020-87
Preprint. Discussion started: 17 April 2020

The Cryosphere Discussions
Open Access
EGU

Table 3. Correlations of mean summer (top right) and mean monthly (bottom left) albedo with mean summer and monthly weather and mass balance conditions, Haig Glacier, 2002-2015. Symbols are defined in Tables 1 and 2. Summer correlations are for the glacier-averaged, JJA conditions. For the monthly data, B_s refers to the monthly summer balance (melting minus refreezing), defined as a negative for mass loss. B_n and B_w are not relevant for the monthly data.

	Annual (B_n, B_w) or summer (JJA, all other variables) means or totals								
	α_s	B_w	B_s	B_n	N_{ss}	PDD	T	Q_N	E_m
α_s	—	0.52	0.66	0.76	0.67	–0.35	–0.85	–0.68	–0.60
B_w		—	–0.15	0.47	0.20	0.25	0.09	–0.16	–0.08
B_s	*0.89*		—	0.94	0.73	–0.73	–0.69	–0.91	–0.99
B_n				—	0.70	–0.55	–0.58	–0.86	–0.90
N_{ss}					—	–0.58	–0.58	–0.76	–0.73
PDD	*–0.74*		*–0.89*			—	0.82	0.64	0.80
T	*–0.73*		*–0.88*			*0.97*	—	0.80	0.73
Q_N	*–0.84*		*–0.97*			*0.92*	*0.91*	—	0.89
E_m	*–0.87*		*–0.99*			*0.9*	*0.90*	*0.99*	—
f_E	*–0.66*		*–0.62*			*0.36*	*0.38*	*0.63*	*0.63*

Table 4. Mean albedo values (± 1σ) along the Haig centreline transect during four surveys in summer, 2017: glacier average, and for the subset of sites over seasonal snow and glacier ice. The number in brackets indicates the number of samples for each average. Snow values at three sites on the upper glacier are estimated on August 9.

Date	All sites	Snow	Ice
July 13	0.48 ± 0.04 (33)	0.48 ± 0.04 (33)	—
July 26	0.34 ± 0.15 (33)	0.48 ± 0.05 (16)	0.21 ± 0.07 (17)
August 9	0.23 ± 0.11 (33)	0.41 ± 0.03 (9)	0.17 ± 0.05 (24)
August 22	0.16 ± 0.11 (33)	0.47 ± 0.08 (3)	0.13 ± 0.05 (30)

https://doi.org/10.5194/tc-2020-87
Preprint. Discussion started: 17 April 2020

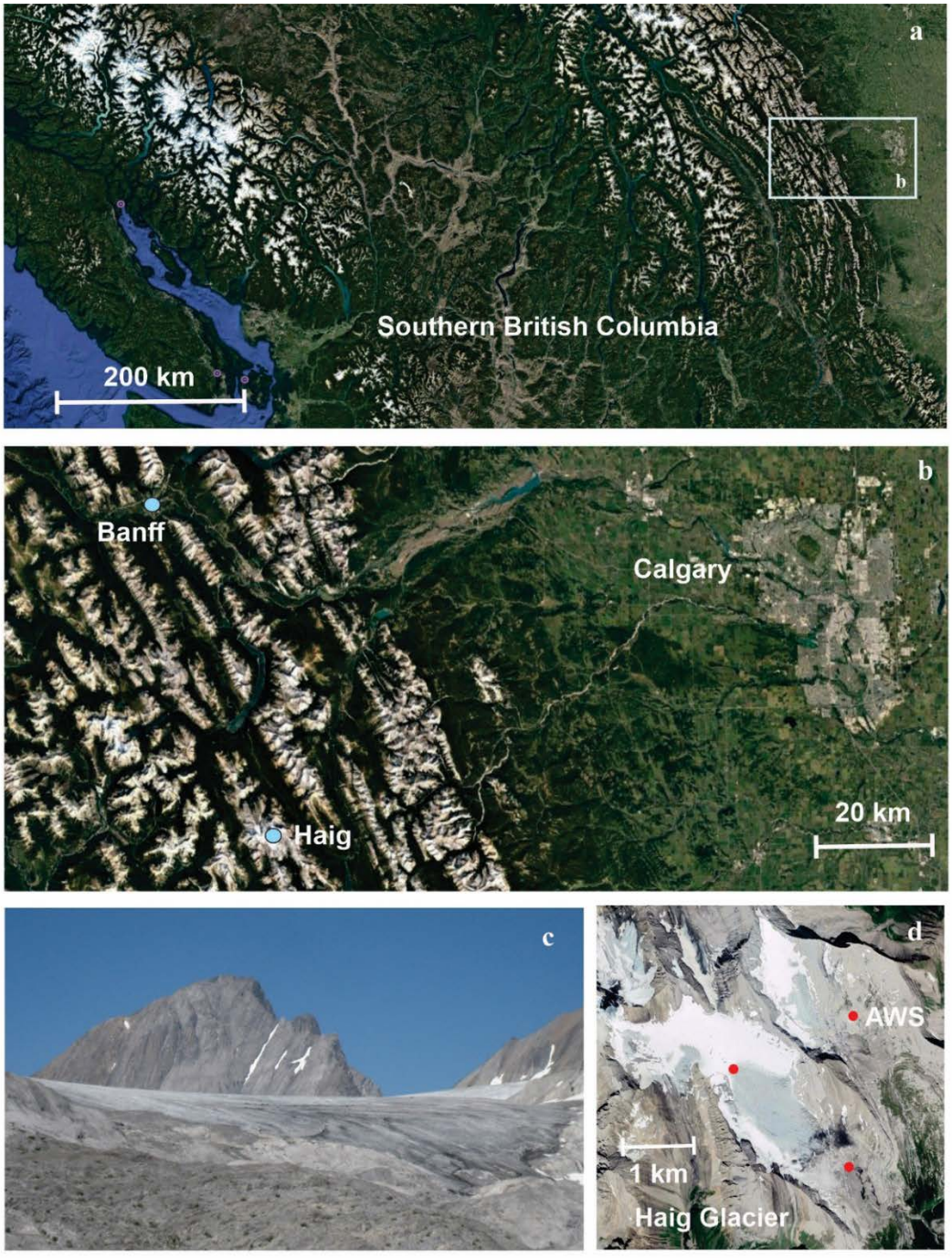

Figure 1. Haig Glacier study area in (a) southwestern Canada. (b) Haig Glacier is about 100 km southwest of Calgary, AB, on the eastern slopes of the Canadian Rocky Mountains. (c) Photograph of the terminus area of the glacier, July 2007, from S. Marshall. (d) Map view of the glacier. Images (a), (b) and (d) are © Google Earth.

https://doi.org/10.5194/tc-2020-87
Preprint. Discussion started: 17 April 2020

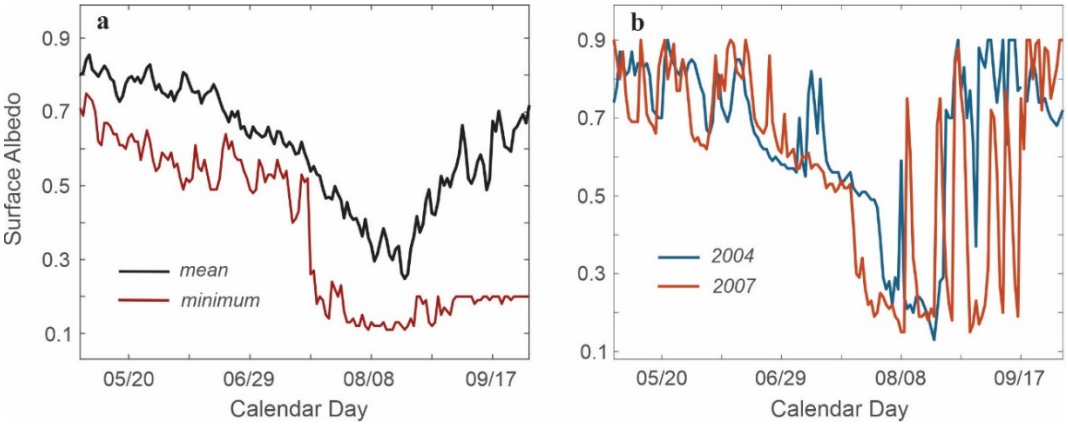

Figure 2. Daily albedo evolution at the Haig Glacier AWS site over the melt season, May to September. (a) Mean and minimum daily albedo from 2002-2016. (b) Select individual years (2004 and 2007) to better illustrate the transition from seasonal snow to exposed glacier ice and the impact of summer snow events (albedo spikes).

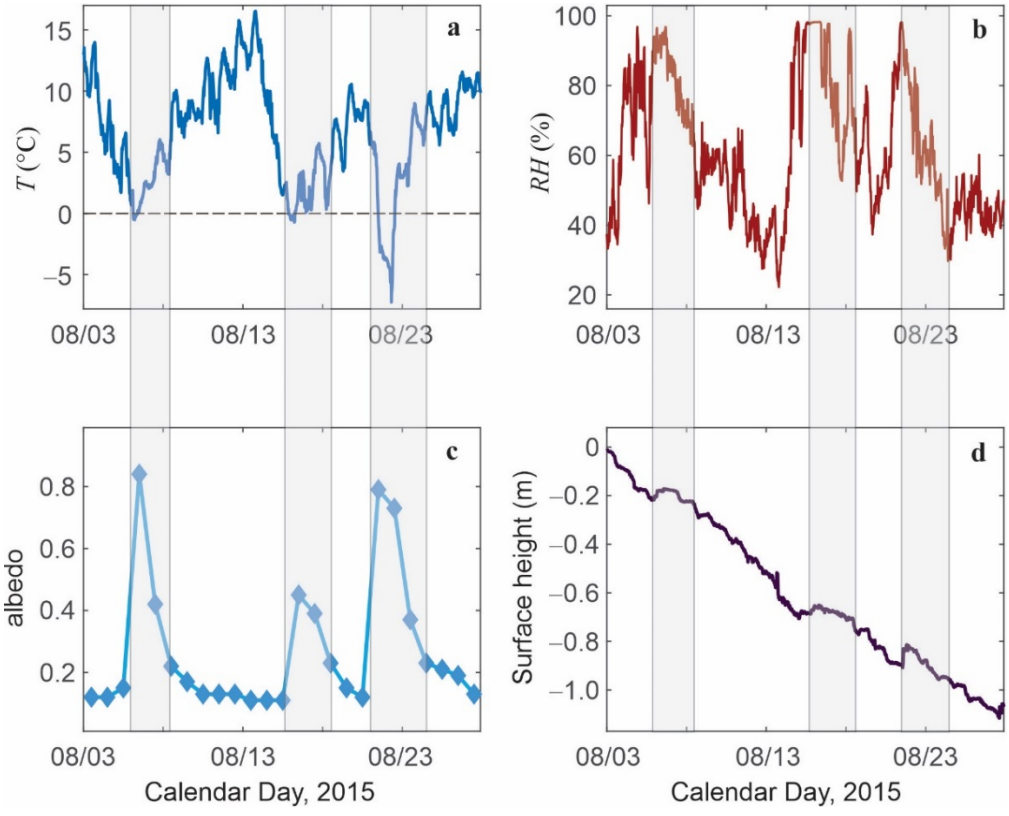

Figure 3. Examples of summer snow events recorded at the Haig Glacier AWS site from August 3-28, 2015. (a) Air temperature, (b) relative humidity, (c) mean daily albedo, and (d) surface height, as measured by the ultrasonic depth gauge (SR50).

https://doi.org/10.5194/tc-2020-87
Preprint. Discussion started: 17 April 2020

845

Figure 4. Photographs of the Haig Glacier, illustrating the variability of summer surface cover. (a) The transition from seasonal snow to exposed glacier ice. (b) Meltwater runnels looking downslope in the ablation area, illustrating the heterogeneous but extensive concentration of surface impurities. (c) Dark ice at the glacier terminus. (d) Fresh snow covering the glacier after a heavy August snowfall. Photos by S. Marshall.

850

https://doi.org/10.5194/tc-2020-87
Preprint. Discussion started: 17 April 2020

The Cryosphere Discussions
Open Access
EGU

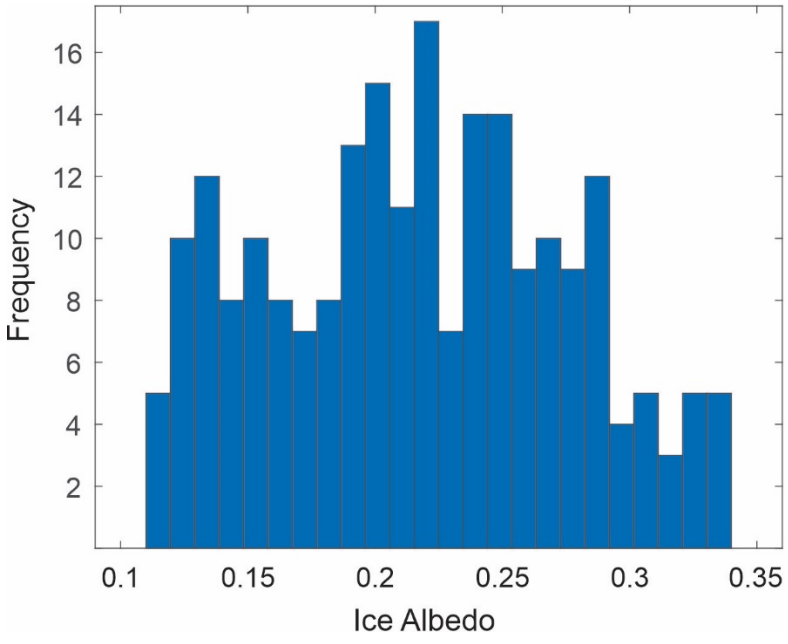

Figure 5. Distribution of ice albedo values recorded at the Haig Glacier AWS from the summers (JJA) of 2002 to 2015 (*N* = 224).

855

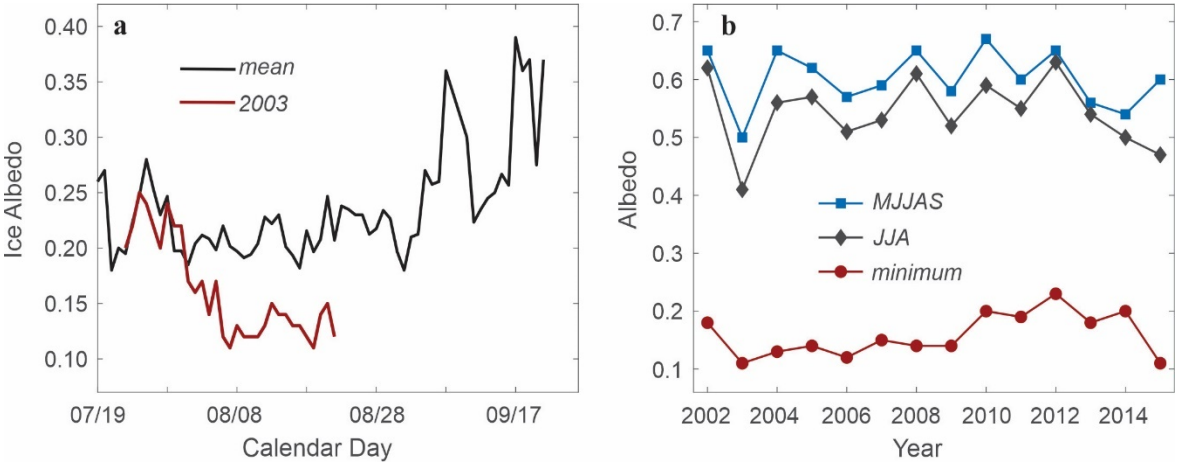

860

Figure 6. (a) Evolution of Haig Glacier ice albedo through the summer melt season. Mean values for 2002-2015 are shown in black and available data from summer 2003 in red. (b) Evolution of the mean melt-season albedo at Haig Glacier from 2002 to 2015, for May through September (blue) and JJA (black). The red line plots the minimum daily value for each year.

865

https://doi.org/10.5194/tc-2020-87
Preprint. Discussion started: 17 April 2020

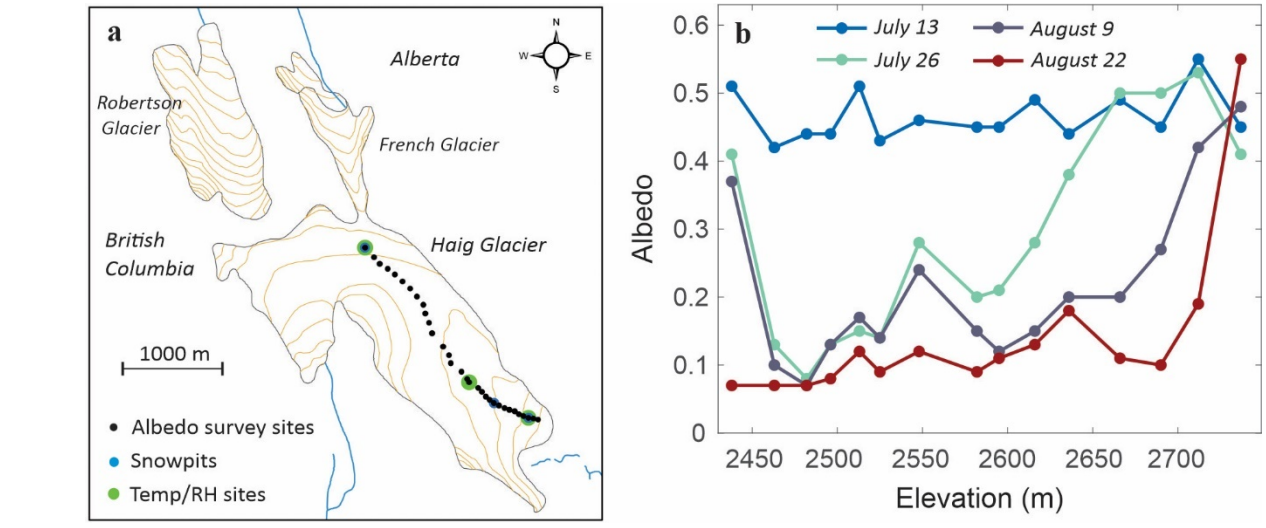

Figure 7. (a) Black circles show the 33 survey sites for winter mass balance and albedo measurements along the Haig Glacier 'centreline' transect. (b) Evolution of surface albedo along the centreline transect during four visits in July and August, 2017.

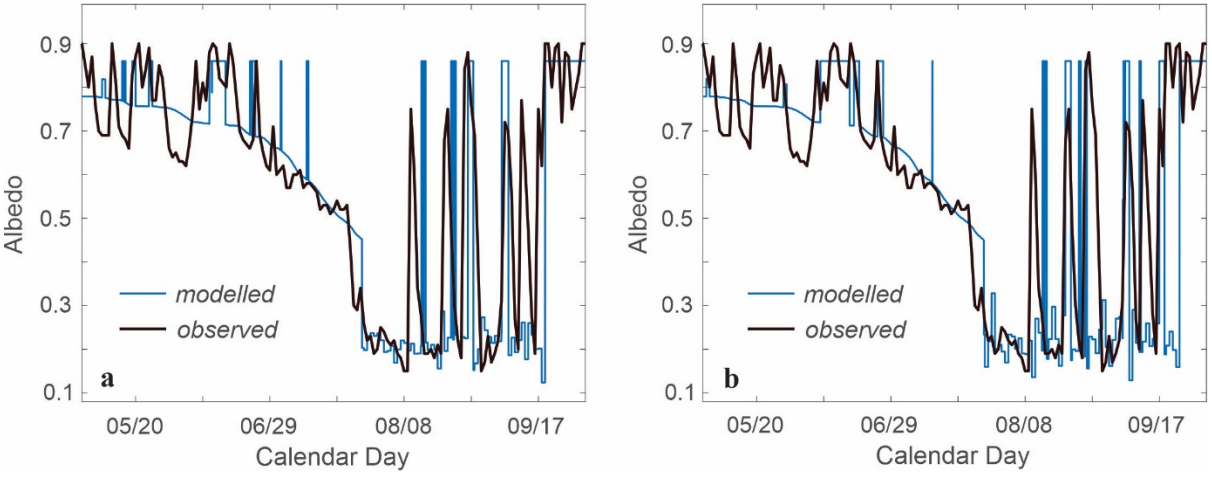

Figure 8. Two realizations of modelled vs. observed surface albedo at the Haig Glacier AWS site, May 1 to September 30, 2007. Summer snow events (albedo spikes) are modelled as random events in the albedo model.

https://doi.org/10.5194/tc-2020-87
Preprint. Discussion started: 17 April 2020

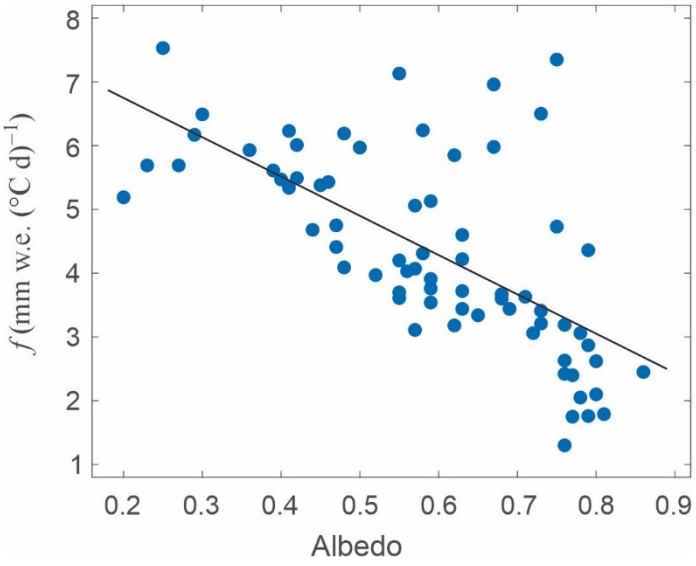

880

Figure 9. Degree-day melt factor, *f*, as a function of monthly mean albedo and melt energy at the AWS site, 2002-2015.